Supplementary material

XPS.

Figure S1a shows the Zr3d spectra of the studied samples. The Zr3d spectrum is known to be a Zr3d_{5/2}–Zr3d_{3/2} doublet, which integral intensities ratio is 3:2. The spinorbit splitting (the difference between the binding energies of $Zr3d_{5/2}$ and $Zr3d_{3/2}$) is 2.4 eV. In this case, the Zr3dspectrum is well described by one doublet. To take into account the effect of sample charging, the spectra were calibrated against the Ce3d u''' line of cerium ($E_{\rm B}$ = 916.7 eV). The binding energy of Zr3d_{5/2} (Table 3) corresponds to zirconium in the oxidized state. For stoichiometric oxide ZrO₂, the binding energy Zr3d_{5/2} lies in the range 182.2-183.3 eV [1-4]. For the catalysts studied, the Zr3d_{5/2} binding energy is 181.5 eV, which can be attributed to zirconium in a state close to Zr3+ [2]. It can be assumed that presence of Pr and Sm cations in PrSmCeZrO2 oxide leads to a decrease in the positive charge on zirconium cations.

Figure S1 also shows the Ce3d spectra of studied catalysts. Cerium is in the Ce^{3+} and Ce^{4+} states. As it is known, the Ce3d spectra have a complex shape (Figure S1b). First, as a result of the spin–orbit interaction, the cerium 3d level splits into two sublevels $Ce3d_{5/2}$ and $Ce3d_{3/2}$, which leads to the appearance of a doublet in the XPS

spectrum, which integral line intensities are in 3:2 ratio. Second, each component of the doublet, in turn, splits into 3 lines in the case of CeO_2 (v/u, v"/u", v"'/u"') or into two lines in the case of Ce_2O_3 (v'/u', V_0/U_0). Having determined the relative intensities of these components, one can estimate the fraction of Ce^{4+} ions [5,6]. In accordance with the results of the spectra decomposition into individual components, for all samples the fraction of Ce^{4+} ions is in the range of 60-75%.

The Pr3d spectra of studied samples are shown in Figure S2a. As it is known, the 3d-level of praseodymium is split into two sublevels $Pr3d_{5/2}$ and $Pr3d_{3/2}$ due to the spin-orbit interaction, the spin-orbit splitting is 20.5 eV. The shape of the Pr3d spectrum has a complex structure consisting of several peaks related to praseodymium in the Pr^{3+} and Pr^{4+} states [5,7]. In accordance with the results of the decomposition of spectra into individual components, the fraction of Pr^{4+} ions for all samples is in the range of 75–85%.

The Sm3d spectra of the studied samples are also shown in Figure S2b. As is known, the 3d-level of samarium is split into two sublevels $\text{Sm}3d_{5/2}$ and $\text{Sm}3d_{3/2}$ due to the spin-orbit interaction, the spin-orbit splitting is $27.2\,\text{eV}$, and the shape of the Sm3d spectrum has a complex structure consisting of several peaks, with the binding energy of $\text{Sm}3d_{5/2}$ being $1082.7-1083.0\,\text{eV}$, which corresponds to samarium in the Sm^{3+} state. In the literature, for Sm_2O_3 ,

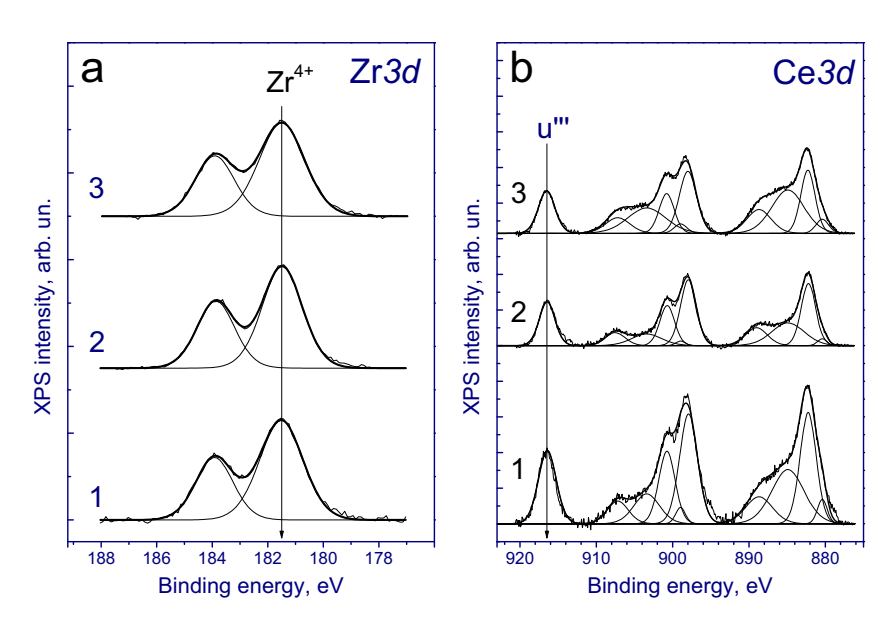


Figure S1: Normalized Zr3d (a) and Ce3d (b) core-level spectra of Sim1 (1), Sim2 (2), and Sim3 (3) catalysts.

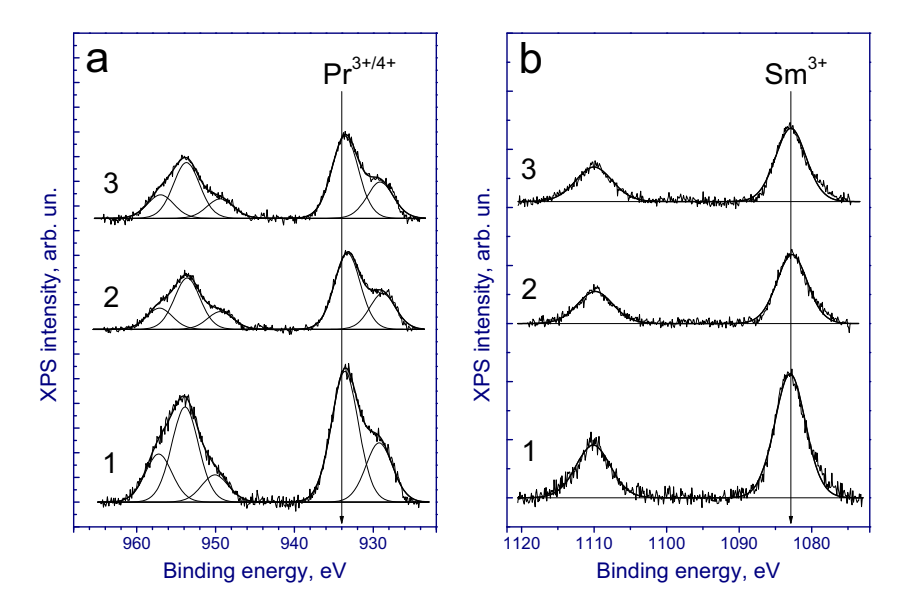


Figure S2: Pr3d (a) and Sm3d (b) core-level spectra of Sim1 (1), Sim2 (2), and Sim3 (3) catalysts. Spectra normalized to the total intensity of corresponding Zr3d spectra.

the values of the binding energy of $\text{Sm}3d_{5/2}$ are given in the range 1082.5-1084.0 eV, while for samarium in the Sm^{2+} state, a lower binding energy is observed [8].

Figure S3 shows the La3d spectra of studied catalysts. As is known, due to spin-orbit interaction, the La3d level splits into two sublevels, which leads to the appearance of the La3d $_{5/2}$ -La3d $_{3/2}$ doublet, the integral intensities of whose components are related as 3:2. In turn, each component in the La3d spectra of lanthanum in the oxidized

state of La^{3+} is accompanied by intense lines of the so-called "shake up" satellites. The spin-orbit splitting (the difference between the binding energies of $La3d_{3/2}$ and $La3d_{5/2}$) is ~16.8 eV. In accordance with the literature data for bulk La_2O_3 , the main peak of $La3d_{5/2}$ is located in the region of 833.2–834.0 eV [9].

For lanthanum carbonate $La_2(CO_3)_3$, slightly higher binding energies of $La3d_{5/2}$ are observed in the range 835.0–835.5 eV [10]. A close value of the $La3d_{5/2}$ binding

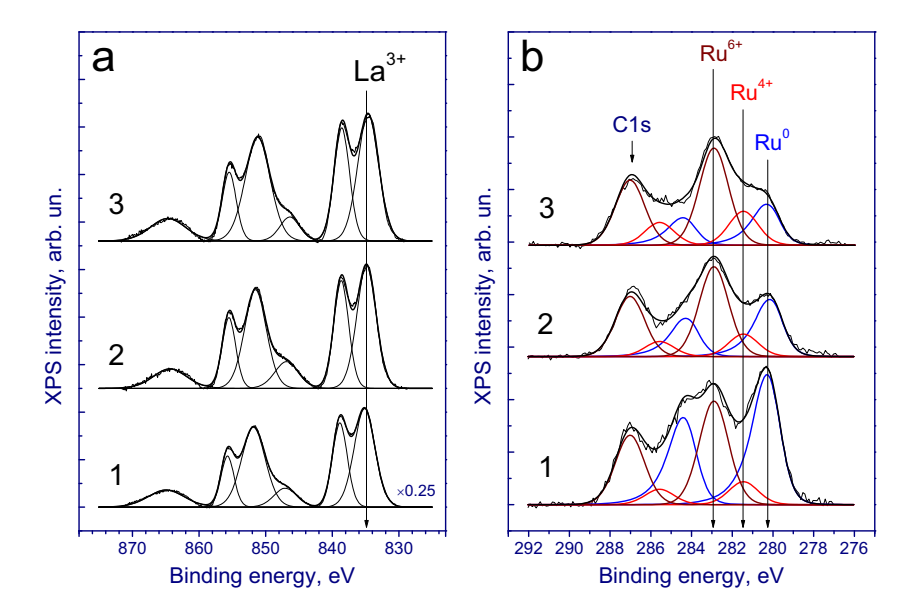


Figure S3: La3d (a) and Ru3d (b) core-level spectra of Sim1 (1), Sim2 (2), and Sim3 (3) catalysts. Spectra normalized to the total intensity of corresponding Zr3d spectra.

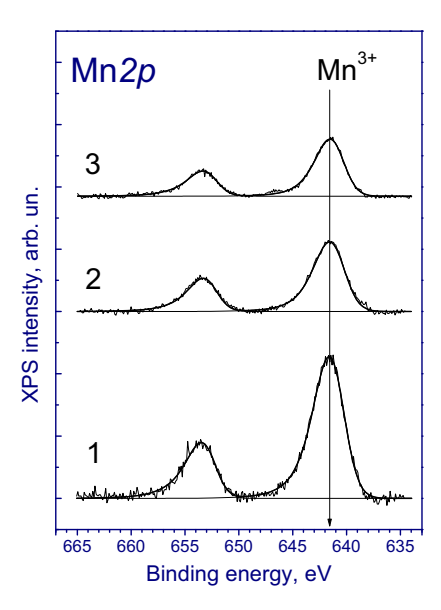


Figure S4: Normalized Mn2p core-level spectra of Sim1 (1), Sim2 (2), and Sim3 (3) catalysts.

energy is observed for lanthanum hydroxides LaOOH and $La(OH)_3 - 834.8 \text{ eV}$ [10]. The observed high binding energy value suggests that lanthanum in the near-surface region is in the form of lanthanum carbonate $La_2(CO_3)_3$.

Figure S3b also shows the Ru3d spectra of studied catalysts. It should be noted that the Ru3d spectrum partially overlaps with the C1s spectrum of carbon (in Figure S3b the contribution from the carbon spectra is subtracted). As is known, the Ru3d spectrum is a Ru3d_{5/2}-Ru3d_{3/2} doublet, which integral intensities ratio is 3:2. The spin-orbit splitting (the difference between the binding energies of Ru3d_{5/2} and Ru3d_{3/2}) is 4.17 eV. Decomposition of spectra into individual components allows us to assert that ruthenium is in three states with binding energies Ru3d_{5/2} in the region of 280.2-280.3, 281.4 and 282.8 eV (Table 4). The first doublet corresponds to ruthenium in the metallic state, the second doublet to ruthenium in the oxidized state Ru⁴⁺; the third doublet is ruthenium in the oxidized state, presumably Ru⁶⁺. According to the literature data, ruthenium in the metallic state is characterized by the Ru3d_{5/2} binding energy in the range of 279.8–280.3 eV. For the Ru^{4+} state,

which is a part of RuO₂ oxide, the Ru3d_{5/2} binding energy lies in the range 280.5–281.4 eV, for RuO₃ oxide, the $Ru3d_{5/2}$ binding energy is in the region of 281.8–282.6 eV [11]. Decomposition of the spectra into individual components makes it possible to estimate the fraction of ruthenium in the metallic state, which for studied catalysts is in the range of 25-50%.

Figure S4 shows the Mn2p spectra of studied samples. The Mn2p spectrum is Mn2p_{3/2}-Mn2p_{1/2} doublet, the integrated line intensities of which are in the 2:1 ratio. To elucidate the manganese state, the binding energy of the Mn2p_{3/2} peak is used, as well as the presence and position of shake-up satellites [12], while the asymmetric shape of the main peaks Mn2p_{3/2} and Mn2p_{1/2} is determined by multi-electron processes. The binding energy of the Mn2 $p_{3/2}$ peak is 641.8. In the literature, for manganese in the composition of oxides MnO, Mn₂O₃, and MnO₂, the binding energies Mn2p_{3/2} are given in the ranges 640.4-641.7, 641.5-641.9, and 642.2-642.6 eV, respectively [13]. Thus, it can be concluded that manganese in the studied catalysts is predominantly in the Mn³⁺ state.

References

- Bulavchenko OA, Vinokurov ZS, Afonasenko TN, Tsyrul'nikov PG, Tsybulya SV, Saraev AA, et al. Reduction of mixed Mn-Zr oxides: in situ XPS and XRD studies. Dalton Trans. 2015:44:15499-507. doi: 10.1039/C5DT01440A.
- Tsunekawa S, Asami K, Ito S, Yashima M, Sugimoto T. XPS study of the phase transition in pure zirconium oxide nanocrystallites. Appl Surf Sci. 2005;252:1651-6. doi: 10.1016/ j.apsusc.2005.03.183.
- Jeon TS, White JM, Kwong DL. Thermal stability of ultrathin [3] ZrO₂ films prepared by chemical vapor deposition on Si(100). Appl Phys Lett. 2001;78:368-70. doi: 10.1063/1.1339994.
- Kim MS, Ko YD, Hong JH, Jeong MC, Myoung JM, Yun I. Characteristics and processing effects of ZrO₂ thin films grown by metal-organic molecular beam epitaxy. Appl Surf Sci. 2004;387-98. doi: 10.1016/j.apsusc.2003.12.017.
- [5] Borchert H, Frolova YV, Kaichev VV, Prosvirin IP, Alikina GM, Lukashevich AI, et al. Electronic and chemical properties of nanostructured cerium dioxide doped with praseodymium. J Phys Chem B. 2005;109:5728-38. doi: 10.1021/jp045828c.
- Christou SY, Álvarez-Galván MC, Fierro JLG, Efstathiou AM. Suppression of the oxygen storage and release kinetics in Ce_{0.5}Zr_{0.5}O₂ induced by P, Ga and Zn chemical poisoning. Appl Catal B. 2011;106:103-13. doi: 10.1016/ j.apcatb.2011.05.013.
- Florea M, Postole G, Matei-Rutkovska F, Urda A, Neatu F, Massin L, et al. Influence of Gd and Pr doping on the properties of ceria: texture, structure, redox behaviour and reactivity in CH₄/H₂O reactions in the presence of H₂S. Catal Sci Technol. 2018;8:1333-48. doi: 10.1039/C7CY02192E.
- Biesinger MC, Lau LWM, Gerson AR, Smart RSC. Resolving [8] surface chemical states in XPS analysis of first row transition metals, oxides and hydroxides: Sc, Ti, V, Cu and Zn. Appl Surf Sci. 2010;257:887-98. doi: 10.1016/j.apsusc.2010.07.086.
- Ramana CV, Vemuri RS, Kaichev VV, Kochubey VA, Saraev AA, Atuchin VV. X-ray photoelectron spectroscopy depth profiling of La₂O₃/Si thin films deposited by reactive magnetron sputtering. ACS Appl Mater Interfaces. 2011;3:4370-3. doi: 10.1021/am201021m.
- [10] Ledford JS, Houalla M, Proctor A, Gercules DM, Petrakis L. Influence of lanthanum on the surface structure and carbon

- monoxide hydrogenation activity of supported cobalt catalysts. J Phys Chem. 1989;93:6770–7. doi: 10.1021/j100355a039.
- [11] Kungurova OA, Khassin AA, Cherepanova SV, Saraev AA, Kaichev VV, Shtertser NV, et al. δ-Alumina supported cobalt catalysts promoted by ruthenium for Fischer-Tropsch synthesis. Appl Catal A. 2017;539:48–58. doi: 10.1016/j.apcata.2017.04.003.
- [12] Feng X, Cox DF. Na deposition on MnO(100). Surf Sci. 2016;645:23–9. doi: 10.1016/j.susc.2015.10.041.
- [13] Jadhav PR, Suryawanshi MP, Dalavi DS, Patil DS, Jo EA, Kolekar SS, et al. Design and electro-synthesis of 3-D nanofibers of MnO_2 thin films and their application in high performance supercapacitor. Electrochim Acta. 2015;176:523–32. doi: 10.1016/j.electacta.2015.07.002.